Egyptian Journal of Chemistry
http://ejchem.journals.ekb.eg/

Preparation of Cobalt Oxide Nanoparticles by Atmospheric Plasma jet and Investigation of Their Structural Characteristics

Kadhim A. Aadim,[a] Ibrahim K. Abbas[b,*]
[a , b] *Department of Physics, College of Science, University of Baghdad, Baghdad, Iraq*

Abstract
In this paper, atmospheric-pressure plasma jet is used to prepare cobalt oxide nanoparticles (Co_3O_4 NPs) within two periods of time which are 10 and 12 minutes and high constant voltage (H.V) supplied by a 21 kV power supply with 3 L/min flow rate of argon and the frequency of 6 kHz DC. current. X-Ray diffraction (XRD) spectrum analysis showed of semi crystalline Co_3O_4 NPs and appearance of a number of different small peaks which observed at 2θ° with particle size 52.987 in 10 minutes and 48.478 nm for 12 minutes. Atomic force microscopy (AFM) was used to demonstrate the coordination of the synthesised Co_3O_4 NPs, the average diameter particle size measured was 22.72 nm and 25.78 nm for 10 and 12 minutes respectively, and showed a high extraordinary topographic contrast. Field Emission Scanning Electron Microscopy (FE-SEM) images demonstrated the topography and morphology of the produced Co_3O_4 NPs where the size of these nanoparticles formed ranged between 10-30 nm, also high resolution transmission electron microscopy (HR-TEM) images revealed a homogenous Co_3O_4 NPs prepared in both preparation time (10, 12) minutes and clear that the formation of dispersed spherical nanoparticles resembles the interconnected grid.

Keywords: Co_3O_4 NPs AFM; Co_3O_4 NPs; Cobalt Oxide Plasma Jet; Co_3O_4 NPs XRD; Co_3O_4 NPs FE-SEM; TEM Co_3O_4 NPs.

1. Introduction

The use of atmospheric pressure plasmas in a wide range of applications in the biological, nanotechnology, and agricultural fields has recently piqued interest[1]. This is particularly true in the biomedical field, where applications include bacteria inhibition, tissue regeneration, and dental bleaching [2]. Research into the properties of atmospheric plasma processes with the goal of determining whether they can be used for nanoparticle preparation, sterilization and disinfection treatment[3]. As well as for protecting industrial materials, equipment, and electronics from biological damage and microbiologically induced corrosion, has become increasingly important in recent years[4,5]. Plasma treatment of living tissues produces the desired therapeutic effect in the sterilization and arrest of bleeding, bleeding control, and cure of certain skin diseases, among other applications[6]. As a result of the increasing need from mankind for new high-productivity sterilization and disinfection technologies that do not require high temperatures and are simple to operate, this trend has taken on a significant amount of significance in recent years[1]. As a result of their distinct features as compared with their bulk equivalents, nanomaterials have attracted a significant deal of attention in recent years[7]. Nanomaterials, which are incredibly small in size and have a large surface area, have demonstrated significant biological activity in the human body[8]. A wide range of uses for Co_3O_4 NPs in biomedicine include medication delivery, cancer therapy, and bioimaging[9]. Nanomaterials are essential in the field of biomedicine[10]. In spite of this, our present understanding of nanomaterials' behavior in relation to human health is still insufficient[11]. Previous research on cobalt systems demonstrated that the synthesis conditions influence phase development, resulting in either single or mixed phases, as a result,

*Corresponding author e-mail: Ibrahim.kareem1104a@sc.uobaghdad.edu.iq.; (Ibrahim K. Abbas).
Receive Date: 01 July 2022, Revise Date: 30 July 2022, Accept Date: 08 August 2022.
DOI: 10.21608/EJCHEM.2022.146951.6414

while synthesizing Co_3O_4 NPs, three critical factors must be considered: (i) the synthesis temperature, (ii) the chemical environment (solvents), and (iii) the crystallite size of the Co_3O_4 NPs, when low-temperature procedures are used, it is discovered that a single exclusive phase production is likely, but a mixture of phases is likely when high-temperature methods are used, bulk cobalt crystallizes in two phases under typical conditions: hexagonal closed packing (hcp) and face-centered cubic (fcc)[12]. Due to its distinctive characteristics when compared to solid, liquid, and gas phase synthesis methodologies, plasma technology is currently getting significant interest as a prominent "green" synthesis method for nanomaterials[13]. Co_3O_4 NPs are often synthesized via many techniques like, spray pyrolysis, ultrasound device, Dc magnetron, and sputtering coating, Co_3O_4 NPs could be efficient nanoparticles as they have good catalytic activity, many efforts have been directed in recent years to the production of Co_3O_4 nanostructures with various morphologies such as nanoparticles, hollow spheres, nanorods, nanoplates, nanowires, nanotubes, and nanocubes, as well as nanoporous structures, Co_3O_4 NPs have been created using a variety of physical and chemical processes, including combustion, microwave irradiation, and atmospheric plasma jet[14]. Co_3O_4 NPs, nanodots, or nanopowder are spherical black particles with a large surface area that are high in surface area[15]. Nanoscale Co_3O_4 NPs have a specific surface area (SSA) in the range of 30 - 70 m^2/g and are typically 20-60 nanometers (nm) in diameter[9]. It is also possible to obtain Nano Cobalt Particles that have been passivated, as well as Ultra High Purity and High Purity Nano Cobalt Particles that have been carbon-coated, magnetic, disseminated, or monodispersed forms[16]. Surface functionalized nanoparticles enable the particles to be preferentially adsorbed at the surface interface by chemically attached polymers, resulting in the particles being retained at the surface interface[8]. The plasma jet is a new and improved design[17]. It was created for this atmospheric plasma system in order to extend the plasma plume at a long distance away from the discharge site, allowing for the treatment of the sample from a remote location in the atmosphere[18]. In this application, the variety of reactive oxygen and nitrogen species (RONS) created by non-thermal atmospheric pressure plasma sources is critical because they are the key to the process[19]. Due to the fact that the chemistry of liquid is influenced by the RONS created by plasma, plasma-liquid interactions play a significant role in the development of nanomaterials[20]. Superoxide, hydroxyl radicals, singlet oxygen, nitric oxide, ozone, and hydrogen peroxide are some of the most common reactive oxygen species (RONS) generated during plasma-liquid interactions[21]. A large concentration of RONS can be produced by atmospheric plasma because of the inherent advantages of working in air[22,23]. Non-thermal plasma has the potential to kill cancer cells either directly or indirectly[24]. Increased specificity and efficiency of treatment can be achieved by the use of conjugated or unconjugated NPs[25]. There have been numerous studies in which researchers have used antibody-conjugated nanoparticles (NPs) to increase cell death and decrease the viability of cancer cells[26]. In the future, this combined technique may prove to be a viable therapeutic option for treating a variety of malignancies and tumors of various types[27]. Recently, non-thermal atmospheric pressure plasma with Co_3O_4 was also used for killing microbes[14]. Non-thermal plasma efficiently kills oral bacteria on agar plates; however, it has less effect on the tooth surface[28]. Therefore, we used APJS to synthesise Co_3O_4 NPs at different times and study the structural properties of these nanoparticles. However, combination treatment with plasma and Co_3O_4 causes significant cell damage, causing loss of intracellular components from many bacterial cells, hence the death of bacteria[16].

2. Experimental:

2.1. Initialization of the Atmospheric Plasma Jet System and Preparation of Co_3O_4 NPs

figure-1 demonstrates a plasma system (APJS) that operates at atmospheric working by argon gas and is used to prepare Co_3O_4 NPs at 21 kV with a frequency of 6 kHz, a 99.99% percent pure cobalt sheet purchased from (THE BRITISH DRUG HOUSES LTD./LONDON, Manufactured in England, 652247/470611). The gas flows through the gas bottle and is controlled by a flowmeter (1-5) L/min, particular plasma needle has an outside diameter of 3 mm and a stainless design, connected it the cathode electrode of the H.V. power supply, and the other electrode is linked to the anode in high-purity cobalt metal in a beaker 10 mL with distilled water. The cobalt sheet dimensions were 1 cm wide and 7 cm long, the beaker contains 7 mL of distilled water and

the length of the cobalt sheet immersed in distilled water was 5 cm, and the distance between the anode electrode and the cathode electrode connected to the tip of the plasma needle was 1 cm. The plasma jet is placed approximately 2 cm away from the surface of the distilled water in the beaker, where the argon gas molecules interact with the distilled water inside the beaker, producing a series of chemical reactions with the metal surface, which results in a change in the color of the liquid to a different color depending on preparation time and the formation of Co_3O_4 NPs (10, 12 min.), This investigation involved the creation of Co_3O_4 NPs with an argon flow rate of 3 L/min and a voltage of 21 kV at various periods of time as shown in the figure-2. The characterisation of the produced Co_3O_4 NPs was carried out in Iran at the University of Kashan for XRD (XPERT PAANALTICAL PHILLIPS HOLLAND), FE-SEM, EDX (TESCN MIRA3 FRENCH), and TEM analyzing.

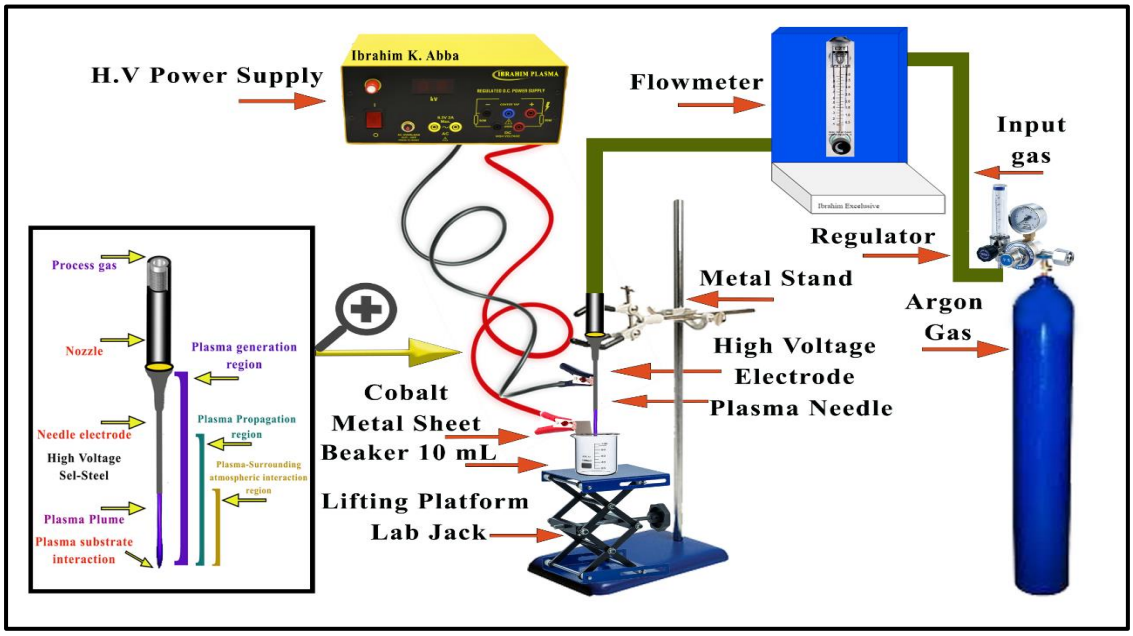

Figure (1): Schematic of Experimental Setup of Atmospheric Plasma Jet for Preparation Co_3O_4 NPs.

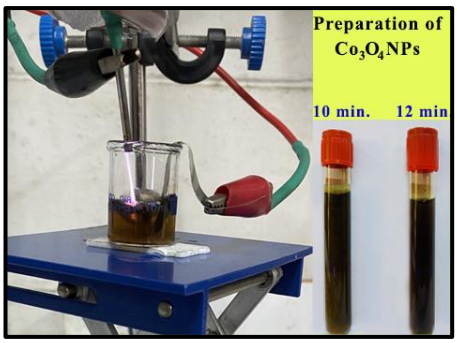

Figure (2): Synthesis of Co_3O_4 NPs by Atmospheric Plasma Jet at 10 and 12 minutes.

3. Results and Discussion:

3.1. Investigation of the Crystal Structure

XRD spectrum of Co_3O_4 NPs prepared by non-thermal plasma at a voltage of 21 kV with a flow of 3 L/min of argon gas in (10, 12) minutes at a distance of 2 cm, where it appears in the figure is an agreement with the spectrum of reference card no. (00-050-1732) which represent of cobalt oxide structure (Co_3O_4 NPs) amorphous or semi crystalline that have crystal system is rhombohedral, the diffraction angular range (2θ°) was between 10° and 80° degrees with appearance of a number of different small peaks which observed at 2θ°= (19.30°) (21.38°) (24.23°) (36.78°) (45.03°) (63.33°) corresponding to (122), (131), (222), (011), (101) and (331) as shown in figure-3, as it represents the phase of Co_3O_4 NPs after preparing it by plasma in

the form of a distilled water for 10 and 12 min. The apparent peaks in the figure also confirm its agreement with the research and literature published by other researchers to prepare Co_3O_4 NPs [13-16]. And Scherrer's equation were used in order to calculate an average size of crystallites[29]. Where the size of the prepared Co_3O_4 NPs is estimated to be about 52.987±10.63 nm at 10 minutes and 48.478±5.30 nm at 12 minutes. Where it became clear through the results that the increase in the preparation time of nanoparticles from 10 to 12 minutes led to a slight decrease in the average diameter particle size of Co_3O_4 NPs, and the reason for this is an increase in the interactions that occur in the baker between (argon atoms flowing through the plasma nozzle + water + submerged cobalt metal + free electrons on the metal surface + oxygen or atmospheric air) all of these factors participate in the formation of nanoparticles, so we have created nanoparticles in water and as a result, this leads to a change in the color of the liquid to a much darker color, as the effect of increasing time this led to the uprooting and formation of these nanoparticles with slightly smaller diameters and sizes. The figure also shows that the highest peak is (131) compared to other peaks, where the anisotropy increases with the increase in particle size, in addition to that, the presence of stacking errors may reduce a coherent scattering area along the direction or at the top (131) compared to other directions, as well exactly the same is demonstrated by the high-resolution TEM images of Co_3O_4 NPs prepared in plasma[23].

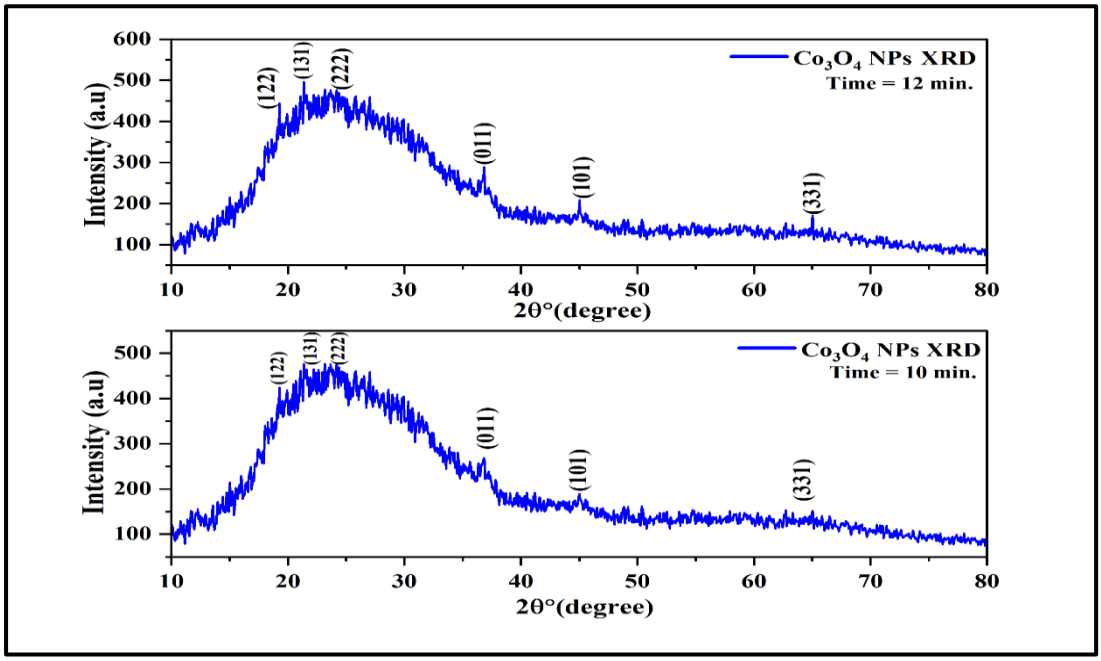

Figure (3): Schematic of XRD for Co_3O_4 NPs Prepared by Plasma jet at (10, 12) min.

3.2. Atomic Force Microscope of Co_3O_4 NPs

The results showed formation of nanorods morphology with some much small spherical Co_3O_4 NPs as shown in the figure-4 and figure-5, the average diameter 25.78 nm with average particle size 13.22 nm and roughness 5.88 nm in 10 minutes as indicted in figure-4, and average diameter of Co_3O_4 NPs nanorods was 22.72 nm and the average particle size was 11.05 nm with roughness 5.762 nm and root mean square Rms (grain-wise) is 2.75 nm in 12 minutes as shown in figure-5, and, also figure-4 indicates the particle size distribution plots of Co_3O_4 NPs average particle size distribution 46.86 nm in 10 minutes as shown in figure-4, whereas Co_3O_4 NPs prepared at 12 minutes, the particle size distribution ranged from 20 to 40 nm with mean value of 38 nm. Since decomposition occurs very rapidly in solution during the interaction of gas molecules emerging from the plasma nozzle with the Co_3O_4 plate the resulting clusters have regular sizes and are consistent or symmetrical in shape[30,31].

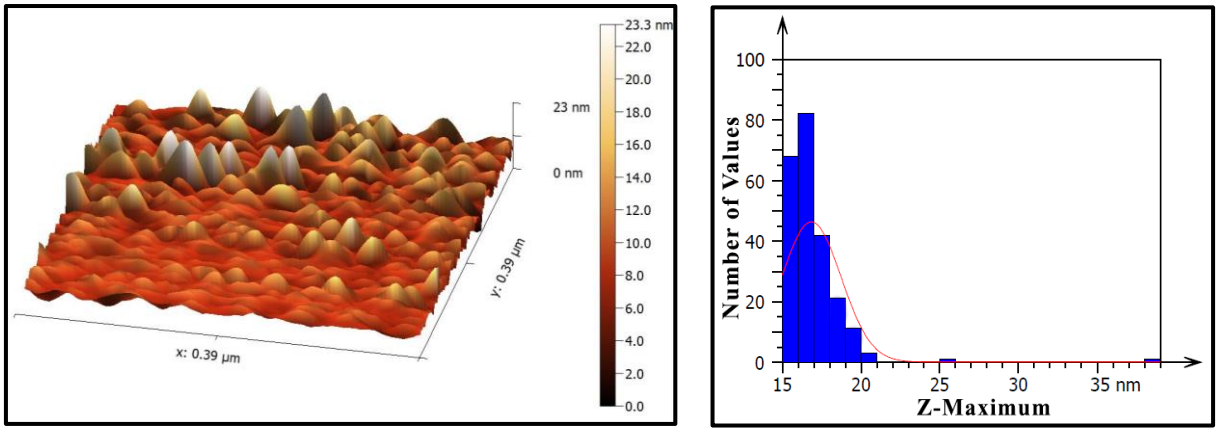

Figure (4): Schematic of AFM for Co_3O_4 NPs and Histogram Prepared by Atmospheric Plasma at 10 minutes.

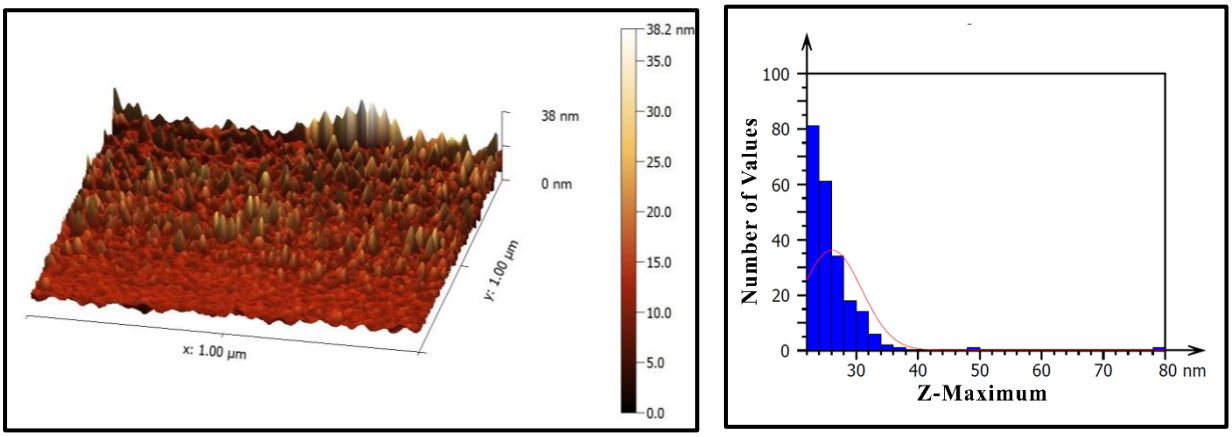

Figure (5): Schematic of AFM for Co_3O_4 NPs and Histogram Prepared by Atmospheric Plasma at 12 minutes.

3.3. Surface Morphological Investigation FE-SEM and EDX of Co_3O_4 NPs

In Figure-6 and figure-7 shows the exact structure of the microscopic surface structure and EDX in figure-8 for concentration of elements in solution of Co_3O_4 NPs, where FE-SEM was used to know the surface morphology of the Co_3O_4 NPs prepared by plasma jet[32]. The images show the magnification that was adopted in this FE-SEM of Co_3O_4 NPs with the attached figure-8 showing the EDAX spectra that are closely related to this prepared Co_3O_4 NPs sample. Through the images and zoom view, it becomes clear to us an interesting fact, which is that the nanostructure of Co_3O_4 NPs is somewhat similar to agglomerate as flowers and small spherical spheres at scaled 100 and 200 nm, and this indicates the homogeneity of the nanoparticles during the preparation of the Co_3O_4 NPs sample, where the size of these nanoparticles formed ranged between 10-30 nm. The spectra of the EDX analysing showed that the apparent spectra belonged to cobalt and oxygen with different concentrations at both the time of Co_3O_4 NPs preparation. EDX spectra of Co_3O_4 NPs prepared by plasma jet indicate the presence of other elements with the cobalt element, namely oxygen and carbon, it is almost certainly derived from the glass substrate and the SEM chamber, as all of these elements have a role in the process of forming Co_3O_4 NPs during their interaction with the liquid at the nozzle of the plasma jet as well as being in good accord with XRD results as shown in figure-8[34]. This suggests that lengthening the preparation period of nanoparticles by atmospheric plasma jet affords the ability to construct very tiny structures from the elements nanoparticles, which is consistent with prior findings[33].

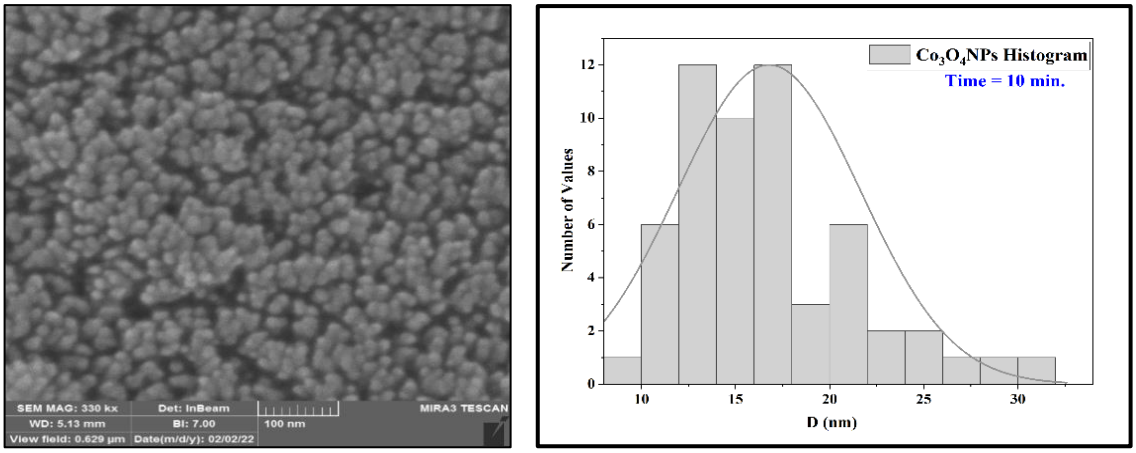

Figure (6): FE-SEM Images of Co_3O_4 NPs Prepared by Plasma Jet at 10 minutes.

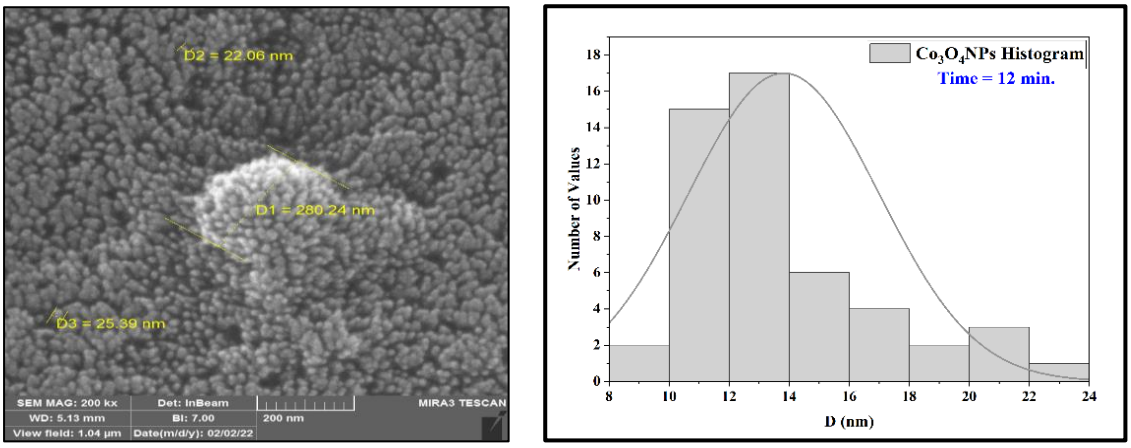

Figure (7): FE-SEM Images of Co_3O_4 NPs Prepared by Plasma Jet at 12 minutes.

3.4. Investigation Transmission Electron Microscopy of Co_3O_4 NPs Surface

Figure-9 shows two pictures of Co_3O_4 NPs at the scale of 300 nm and 150 nm. It is clear form photos, that the formation of dispersed spherical oxide nanoparticles Co_3O_4 resembles the interconnected grid. The average diameter of the Co_3O_4 nanoparticles ranges from 10 to 30 nm, with a narrow size distribution ranged from 10 to 20 nm. and the presence of some large particles represents the bonding and agglomeration of these Co_3O_4 NPs, and when compared with FE-SEM results, we note the agreement of these values obtained with the results in the TEM image. A small sphere-like shape with a restricted size distribution based on the TEM pictures, it is possible to conclude that this synthesis procedure of plasma jet is suitable for obtaining very tiny Co_3O_4 nanoparticles. The particle size distribution of the Co_3O_4 nanoparticles has also been examined using TEM analyzing. We found that increasing the preparation time to 12 minutes' results in the formation of spherical morphology with some spherical Co_3O_4 NPs. The considerable difference in size between the SEM and TEM observations and the manufacturer's value is assumed to be owing to the difference in size between the particles and the crystallite, according to the manufacturer's data. As determined by FE-SEM, a nanoparticle is an agglomeration comprised of two or more individual crystallites, with the size of the nanoparticle being larger than the size of an individual crystallite as estimated by the Debye–Scherer equation from the XRD pattern[35]. Particle size is a critical physical component that influences the fate of Co_3O_4 NPs in the environment, as demonstrated by these findings[9-11]. The combination of results based on a variety of biological activities and physicochemical properties, rather than a single activity and property, would be more useful in assessing the toxicity of NPs in

ecosystems than a single activity and property alone.

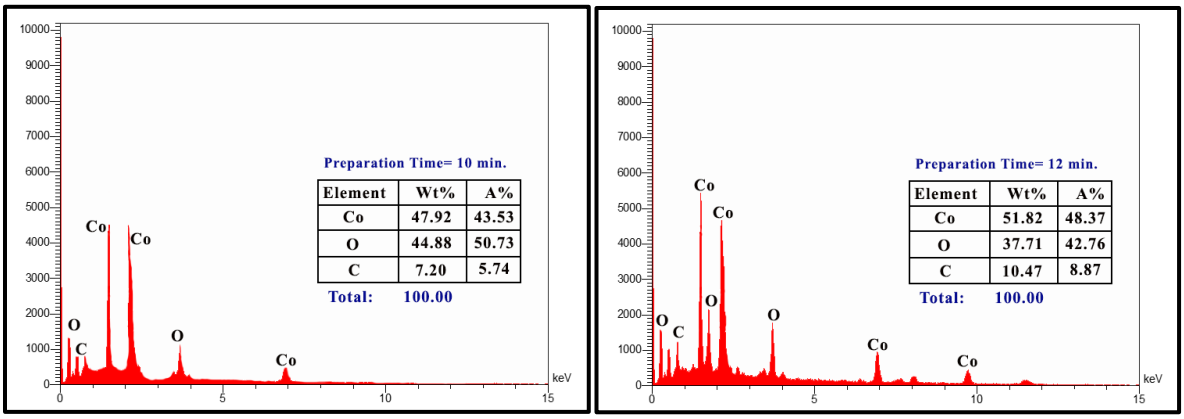

Figure (8): EDX Spectrum of Co_3O_4 NPs Prepared at 10 and 12 minutes.

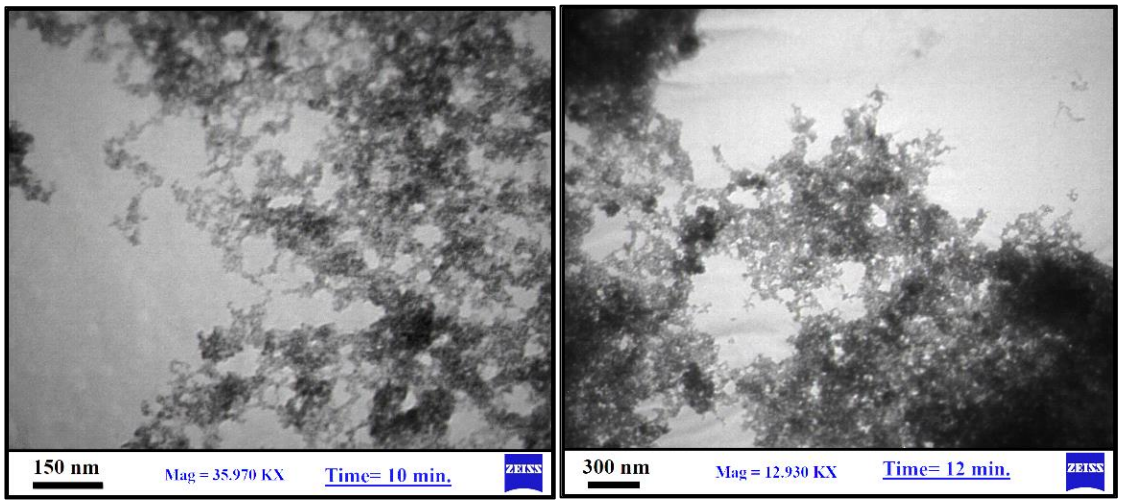

Figure (9): TEM image of Co_3O_4 NPs Prepared by Plasma Jet Scaled at 300 nm and 150 nm in (10, 12) minutes.

4. Conclusions

The results showed after preparing the nanoparticles of Co_3O_4 for (10, 12) minutes, (XRD) analysing showed that Co_3O_4 NPs have several small peaks appeared in the radiation spectrum (XRD) which have amorphous or semi crystalline structure, with an average particle size of the prepared Co_3O_4 NPs is 52.987±10.63 nm at 10 minutes and 48.478±5.30 nm at 12 minutes, as well as agglomerate symmetrical nanostructure of Co_3O_4 NPs is somewhat similar to agglomerate as flowers and small spherical spheres at scaled 100 and 200 nm, where the size of these Co_3O_4 nanoparticles formed ranged between 10-30 nm in FE-SEM and TEM images, also the diameter of the Co_3O_4 NPs was about 25.75 nm and 22.72 for (10, 12) minutes respectively as showed in AFM and results showed a high extraordinary topographic contrast of Co_3O_4 NPs, this indicates that increasing the preparation time from 10 minutes to 12 minutes led to a decrease in the average nanoparticle diameter of Co_3O_4 NPs, it demonstrated a strong exceptional topographic contrast. As well as results showed the presence of low different concentrations of some metals in EDX such as carbon for both preparation times (10, 12) minutes.

Acknowledgement

We would like to express our gratitude to and extend our sincere thanks for the plasma laboratory in the physics department of the College of Sciences, Baghdad University. We also offer our gratitude to everyone who inspired us to continue with this work and the pursuit of knowledge.

References

[1]K. S. Kim. and T. H. Kim, Nanofabrication by thermal plasma jets: From nanoparticles to low-dimensional nanomaterials. *Journal of Applied Physics*, **125**, 70901 (2019). https://doi.org/10.1063/1.5060977.

[2]R. Shrestha, D.P. Subedi, J.P. Gurung, C.S. Wong, Generation, characterization and application of atmospheric pressure plasma jet. *Sains Malaysiana*, **45**, 1689–1696 (2016).

[3]M. Laroussi, Low-temperature plasmas for medicine?. *IEEE Transtion Plasma Science*, **37**, 714–725 (2009). 10.1109/TPS.2009.2017267

[4]N.N. Misra, O. Schlüter, P.J. Cullen, Cold plasma in food and agriculture: fundamentals and applications, Academic Press, 2016. https://doi.org/10.1016/C2014-0-00009-3.

[5]K.A. Aadim. and R.H. Jassim, Determination of plasma parameters and nanomaterial's synthesis of Zn and Mn using laser induced plasma spectroscopy. *AIP Conference Proceeding*, **2372**, 80014 (2021). https://doi.org/10.1063/5.0067300.

[6]P.K. Chu, J.Y. Chen, L.P. Wang, N. Huang, Plasma-surface modification of biomaterials. *Materials Science Engenering Reports*, **36**, 143–206 (2002). https://doi.org/10.1016/S0927-796X(02)00004-9.

[7]P. Xie, Y. Qi, R. Wang, J. Wu, X. Li, Aqueous gold nanoparticles generated by ac and pulse-power-driven plasma jet. *Nanomaterials*. **9,** 1488 (2019). https://doi.org/10.3390/nano9101488.

[8]P. Biswas. and C.-Y. Wu, Nanoparticles and the environment. *Journal of Air& Waste Management Association*, **55**, 708–746 (2005). https://doi.org/10.1080/10473289.2005.10464656

[9]A.F. Khusnuriyalova, M. Caporali, E. Hey-Hawkins, O.G. Sinyashin, D.G. Yakhvarov, Preparation of cobalt nanoparticles. *European Journal of Inorganic Chemistry*, **2021**, 3023–3047 (2021). https://doi.org/10.1002/ejic.202100367.

[10]G. Ciofani. Smart nanoparticles for biomedicine, Elsevier, 2018. https://doi.org/10.1016/C2017-0-00984-9.

[11]W.Q. Lim. and Z. Gao, Plasmonic nanoparticles in biomedicine, *Nano Today*, **11**, 168–188 (2016). https://doi.org/10.1016/j.nantod.2016.02.002.

[12]F.H.L. Starsich, I.K. Herrmann, S.E. Pratsinis, Nanoparticles for biomedicine: coagulation during synthesis and applications. *Annual of Review Chemistry and Biomol Engenearing*, **10,** 155–174 (2019).

[13]F. Fang, M. Li, J. Zhang, C.-S. Lee, Different strategies for organic nanoparticle preparation in biomedicine. *ACS Mater of Letter*, **2**, 531–549 (2020). https://doi.org/10.1021/acsmaterialslett.0c00078.

[14]L. Wang, Y. Yi, H. Guo, X. Du, B. Zhu, Y. Zhu, Highly dispersed Co nanoparticles prepared by an improved method for plasma-driven NH3 decomposition to produce H2, Catalysts. 9, 107 (2019). https://doi.org/10.3390/catal9020107.

[15]Y. Song, H. Modrow, L.L. Henry, C.K. Saw, E.E. Doomes, V. Palshin, J. Hormes, C.S.S.R. Kumar, Microfluidic synthesis of cobalt nanoparticles. *Chemistry of Materals*, **18**, 2817–2827 (2006). https://doi.org/10.1021/cm052811d.

[16]A.H. Ashour, A.I. El-Batal, M.I.A.A. Maksoud, G.S. El-Sayyad, S.H. Labib, E. Abdeltwab, M.M. El-Okr, Antimicrobial activity of metal-substituted cobalt ferrite nanoparticles synthesized by sol–gel technique. *Particuology*, **40,** 141–151 (2018). https://doi.org/10.1016/j.partic.2017.12.001.

[17]R.S. Mohammed, K.A. Aadim, K.A. Ahmed, Estimation of plasma parameters in a DC atmospheric pressure Argon plasma jet. *AIP Conference Proceeding*, **2386**, 80050 (2022). https://doi.org/10.1063/5.0066788.

[18]H.R. Humud, A.S. Wasfi, W. Abd Al-Razaq, M.S. El-Ansary, Argon plasma needle source. *Iraqi Journal of Physics*, **10**, 53–57 (2012).

[19]A. Khlyustova, C.P. Labay, Z. Machala, M.P. Ginebra Molins, C. Canal Barnils, Important parameters in plasma jets for the production of RONS in liquids for plasma medicine: A brief review. *Front of Chemistry Science of Engeneering*, **13**, 238–252 (2019). https://doi.org/10.1007/s11705-019-1801-8.

[20]Y. Yang, Y.I. Cho, A. Fridman, Plasma discharge in liquid: water treatment and applications, CRC press, 2017. https://doi.org/10.1201/b11650.

[21]K.A. Aadim. and H.R. Najem, Effect of cold atmospheric pressure plasma needle on DNA. *Journal of Applied Physics*, **7**, 52-55 (2015).

[22]A. George, B. Shen, M. Craven, Y. Wang, D. Kang, C. Wu, X. Tu, A Review of Non-Thermal Plasma Technology: A novel solution for CO2 conversion and utilization, *Renewable and Sustainable Energy Reviews*, **135,** 109702 (2021). https://doi.org/10.1016/j.rser.2020.109702.

[23]X. Xu, J. Wu, W. Xu, M. He, M. Fu, L. Chen, A. Zhu, D. Ye, High-efficiency non-thermal plasma-catalysis of cobalt incorporated mesoporous MCM-41 for toluene removal. *Catalysis Today*, **281,** 527–533 (2017). https://doi.org/10.1016/j.cattod.2016.03.036.

[24]I.K. Abbas. and M.U. Hussein, the Effect of Non-Thermal Plasma Needle on Staphylococcus Aureus Bacteria. *Biochemical and Cellular Archives*, **18**, 5075 (2018).

[25]P.M. Bellan, Fundamentals of plasma physics, Cambridge University Press, 2008.

[26]M.U. Hussein, R.T. Mohsen, Ambient Decontamination by Non-Thermal Plasma in

Atmospheric Pressure Air. *Journal of Physics Conference Series*, **1032**, 012032 (2018). https://doi.org/10.1088/1742-6596/1032/1/012032.
[27]S.K.P. Veerapandian, J.-M. Giraudon, N. De Geyter, Y. Onyshchenko, C. Krishnaraj, S. Sonar, A. Löfberg, K. Leus, P. Van Der Voort, J.-F. Lamonier, Regeneration of Hopcalite used for the adsorption plasma catalytic removal of toluene by non-thermal plasma. *Journal Hazard Materials*, **402** 123877 (2021). https://doi.org/10.1016/j.jhazmat.2020.123877.
[28]I.K. Abbas, M.U. Hussein, H. Muthanna, H.H. Murbat, The Effect of the Non-Thermal Plasma Needle on Pseudomonas Aeruginosa Bacteria, *Iraqi Journal of Science*, **58** 1214–1219 (2017). https://doi.org/10.24996/ijs.2017.58.3a.5.
[29]S. Choi, L.D.S. Lapitan Jr, Y. Cheng, T. Watanabe, Synthesis of cobalt boride nanoparticles using RF thermal plasma. *Advantge of Powder Technolgy*, **25**, 365–371 (2014). https://doi.org/10.1016/j.apt.2013.06.002.
[30]D. Lebedev, N. Nurgazizov, A. Chuklanov, A. Bukharaev, Isolated Cobalt Nanoparticles Prepared on HOPG in Ultrahigh Vacuum Using Thermal Annealing. *Advance of Nanoparticles*, **2**, 236 (2013). http://dx.doi.org/10.4236/anp.2013.23033.
[31]M. Imadadulla, M. Nemakal, L.K. Sannegowda, Solvent dependent dispersion behaviour of macrocycle stabilized cobalt nanoparticles and their applications, *New Journal of Chemistry*, 42, 11364–11372 (2018). https://doi.org/10.1039/C8NJ01773E.
[32]J.N. Appaturi, T. Pulingam, S. Muniandy, I.J. Dinshaw, L.B. Fen, M.R. Johan, Supported cobalt nanoparticles on graphene oxide/mesoporous silica for oxidation of phenol and electrochemical detection of H2O2 and Salmonella spp. *Materials Chemistry of Physics*, **232,** 493–505 (2019). https://doi.org/10.1016/j.matchemphys.2018.12.025.
[33]A. Anwar, L. Chi Fung, A. Anwar, P. Jagadish, A. Numan, M. Khalid, S. Shahabuddin, R. Siddiqui, N.A. Khan, Effects of shape and size of cobalt phosphate nanoparticles against Acanthamoeba castellanii. *Pathogens*, 8 260 (2019). https://doi.org/10.3390/pathogens8040260.
[34]J.-H. Oh, M. Kim, Y.H. Lee, S.-H. Hong, S.S. Park, T.-H. Kim, S. Choi, Synthesis of cobalt boride nanoparticles and h-BN nanocage encapsulation by thermal plasma. *Ceramics International*, **46** 28792–28799 (2020). https://doi.org/10.1016/j.ceramint.2020.08.042.
[35]S. Das, C. Manoharan, M. Venkateshwarlu, P. Dhamodharan, Structural, optical, morphological and magnetic properties of nickel doped cobalt ferrite nanoparticles synthesized by hydrothermal method. *Journal of Materials Science Mater Electron*, **30**, 19880–19893 (2019). https://doi.org/10.1007/s10854-019-02355-0.